

Nanoscale Probing of a Polymer-Blend Thin Film with Tip-Enhanced Raman Spectroscopy

Boon-Siang Yeo, Esther Amstad, Thomas Schmid, Johannes Stadler, and Renato Zenobi*

Fundamental advances have been made in the spatially resolved chemical analysis of polymer thin films. Tip-enhanced Raman spectroscopy (TERS) is used to investigate the surface composition of a mixed polyisoprene (PI) and polystyrene (PS) thin film. High-quality TER spectra are collected from these nonresonant Raman-active polymers. A wealth of structural information is obtained, some of which cannot be acquired with conventional analytical techniques. PI and PS are identified at the surface and subsurface, respectively. Differences in the band intensities suggest strongly that the polymer layers are not uniformly thick, and that nanopores are present under the film surface. The continuous PS subsurface layer and subsurface nanopores have hitherto not been identified. These data are obtained with nanometer spatial resolution. Confocal far-field Raman spectroscopy and X-ray photoelectron spectroscopy are employed to corroborate some of the results. With routine production of highly enhancing TERS tips expected in the near future, it is predicted that TERS will be of great use for the rigorous chemical analysis of polymer and other composite systems with nanometer spatial resolution.

Keywords:

- AFM
- polymers
- surface analysis
- thin films
- tip-enhanced Raman spectroscopy

1. Introduction

Polymer-blend thin films are used in a wide range of devices from microelectronics, light-emitting diodes (LEDs), and high-density information storage media to medical implants.^[1–3] The functionality of these appliances is intimately linked to the interfaces of the polymer blend: the tribology is influenced by the surface, while the bulk properties of the material are often dominated by the interfaces between the various components. A method to tailor-make these surfaces and interfaces is by surface enrichment.^[4] Using this technique, materials can be designed with unique properties.

For example, the surface coating of a nonstick frying pan can be made to stay clean while remaining hardy and durable. Similarly, a tire can be fabricated to exhibit sufficient track gripping without rapid wear. The usability of the polymer films can be extended by the incorporation of nanopores. Such porous structures have attracted great attention because they can be employed as high-performance antireflection coatings or as membranes in separation processes.^[5,6]

Although the bulk properties of polymers, such as their thermal behavior and micromechanical strength, can be easily measured, it remains difficult to analyze their surface and subsurface chemical compositions, especially with high spatial resolutions. This is due to the inadequacy of the traditionally used analytical methods. We illustrate this fact with some examples. Atomic force microscopy (AFM) with its various imaging modes is a commonly used technique for studying polymer surfaces.^[7] Unfortunately, the chemical identity of the polymers cannot be elucidated directly from the images. Entities present at the subsurface of the film, such as nanopores, would also be undetectable. In addition, tapping mode and friction force AFM are known to give imaging artifacts.^[8–10] For example, no frictional contrast was observed

[*] Prof. R. Zenobi, Dr. B.-S. Yeo, Dr. T. Schmid, J. Stadler
Department of Chemistry and Applied Biosciences, ETH Zurich
8093 Zurich (Switzerland)
E-mail: zenobi@org.chem.ethz.ch
E. Amstad
Department of Materials, ETH Zurich
8093 Zurich (Switzerland)

for a polystyrene/poly(methyl methacrylate) mixed film because of strong moisture-induced capillary forces between the tip and sample.

X-ray photoelectron spectroscopy (XPS) is also commonly employed for polymer analysis. It has excellent depth resolution of a few nanometers but the lateral spatial resolution (afforded by standard spectrometers) is inadequate (several micrometers). Thus, when using XPS the location and local concentrations of the components of a heterogeneous polymer film cannot be accurately ascertained.^[4] Both IR aperture and apertureless scanning near-field optical microscopy (SNOM) are promising methods, but usually give absorbance or scattering at selected wavelengths.^[11–14] As a result, chemical interactions that may shift the spectral positions of the vibrational modes are not detected or can be misinterpreted. Moreover, image contrast based on IR aperture SNOM has been demonstrated to be artifact prone, due to other sources of contrast that are nonchemical in nature.^[15]

An inadequate depth resolution is especially problematic. For example, the depth resolution of an increasingly popular technique for polymer analysis, confocal Raman spectroscopy, can be as good as $\approx 1 \mu\text{m}$.^[16–18] However, this resolution is not sufficient for analyzing thin polymer films (e.g., commercially valuable polymer LED films) that are only tens of nanometers in thickness.^[19] Due to polymer segregation and surface enrichment, the chemical compositions of these films can vary tremendously within this small depth. The presence of all possible Raman signals in a spectrum of such a film would imply, in the absence of other data, that either a) the thin film is completely homogeneous or b) it is segregated into separate laminar layers; (a) and (b) cannot be differentiated! Illustrated by the examples presented above and with rapid developments in nanoscience and nanotechnology, the need for an analytical method that can accurately investigate the surface chemical composition of a film with high spatial resolution is clearly no longer a “luxury”, but a real necessity.

Herein, we introduce tip-enhanced Raman spectroscopy (TERS) as a unique analytical method to investigate the surface molecular composition of polymer blends in situ and nondestructively. TERS is essentially a hybrid system that harvests and combines the nanometer resolution afforded by scanning probe microscopy and the molecular fingerprinting available from surface-enhanced Raman spectroscopy (SERS).^[13,20–28] It has been shown both theoretically and experimentally to enhance signals from analytes with lateral and depth resolutions of $\approx 20 \text{ nm}$.^[21,29,30] A strong advantage is its generation of a complete spectrum without the need to tune the excitation wavelength. As a result, band shifts exhibited by the analytes or the presence of other compounds, such as contaminants, can be easily discerned. TERS has mainly been applied to proof-of-principle studies using analytes with strong resonance Raman activities (e.g., dye molecules).^[13,27] We were surprised to discover that the surfaces of polymer thin films have never been investigated with this sensitive technique, although these materials are important both technologically and commercially. An immiscible polystyrene (PS)/polyisoprene (PI) polymer-blend thin film was chosen as the sample in this study. Blended in suitable proportions, these

polymers are employed as components in hot-melt adhesives and sealants, modifiers for general rubber compounding, and can be directly molded into sporting goods.^[31]

A wealth of structural details was revealed from the high-quality tip-enhanced Raman (TER) spectra collected from these mixed PI and PS samples. This is particularly noteworthy because both PI and PS do not exhibit any resonance enhancement and are weak Raman scatterers. It is shown by using TERS that the polymer film is surface-enriched with a layer of PI. A continuous layer of PS was identified at the subsurface. These data also suggest the existence of nanopores at the subsurface of the polymer film. The latter two features have never been previously identified in PI/PS systems. The possibility of forming nanopores in a polymer film through a simple spin-coating process is especially intriguing, since current methods to synthesize such porous materials are usually multistep and require selective dissolution processes, use of polymeric porogens, etc.^[5,6,32] Differences in the local thickness of the PI and PS layers were also found. The performance of TERS is compared with that of confocal Raman spectroscopy. As the former gave more highly spatially resolved chemical information than the latter (lateral resolution: $\approx 20 \text{ nm}$ vs. $\approx 400 \text{ nm}$; vertical: $\approx 20 \text{ nm}$ vs. $\approx 1 \mu\text{m}$), the molecular composition of the PI/PS film was elucidated in much more detail. XPS was employed to support the TERS data. The present results have immediate implications in polymer film technologies.

2. Results

2.1. Confocal Raman Spectroscopy of PI/PS Films

An experimental configuration consisting of an inverted laser-scanning confocal microscope (LSCM), an AFM instrument, and a Raman spectrograph/CCD detector was used (Figure 1).^[20] Light from a 532 nm laser was focused through a 1.4 NA (numerical aperture) objective onto the samples. An AFM image of the sample was first collected by tip scanning.

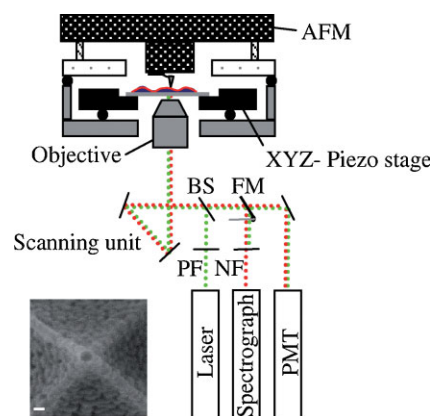


Figure 1. Schematic diagram of the experimental configuration. BS: beam splitter, FM: flipping mirror, PF: plasma filter, NF: notch filter, PMT: photomultiplier tube, AFM: atomic force microscope. A scanning electron microscopy (SEM) image of an Ag-coated tip is shown (scale bar: 25 nm).

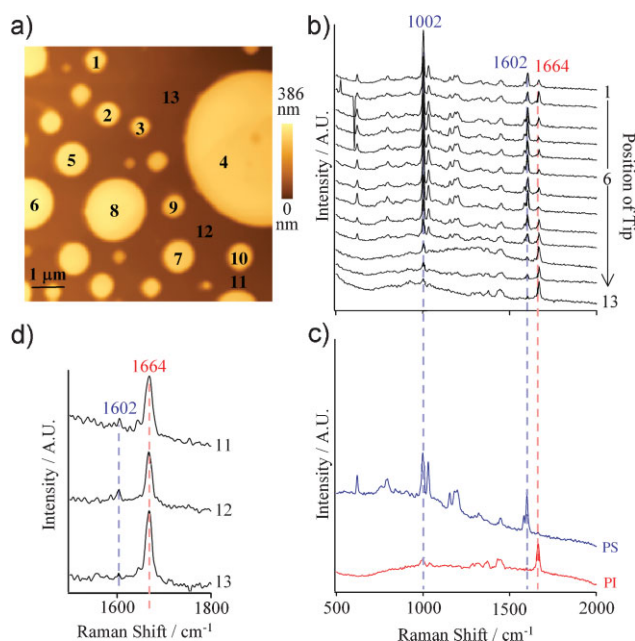


Figure 2. a) AFM topography image of a PI/PS film and b) sequence of confocal Raman spectra collected from the positions depicted in (a). The spikes in spectrum 2 were caused by cosmic rays. c) Raman spectra of pure PS (blue trace) and PI (red trace). d) Zoomed view of spectra 11–13 in (b). Each spectrum was acquired for 120–180 s.

The tip was then parked at a desired spot. Guided by confocal imaging, the tip apex was easily located. Then, 100–150 μW light was focused onto the apex (spot size ≈ 400 nm in diameter) and hence the sample. The backscattered light was channeled into the detector to yield a Raman spectrum. With the exception of the Raman spectra of pure PI and PS, all the Raman/TER spectra are presented in the time order in which they were acquired during an experiment. For example, the spectrum in position 1 is collected before the one in position 2.

Thin PI/PS films were made by spin-coating a PI/PS mixture (1:1) in toluene (2 μL) onto clean glass slides. The AFM image and far-field Raman spectra taken from a PI/PS thin film are presented in Figure 2a and b, respectively. Raman spectra of pure PI and PS are shown in Figure 2c. Circular protrusions mainly 300–1500 nm in diameter can be observed in the topographical image. Since spin-coated pure PI or PS films do not exhibit any well-defined topographical features, these depressions/protrusions must therefore originate from the phenomenon of PI and PS segregation. To confirm this hypothesis, confocal Raman spectroscopy was performed at the depicted positions (1–13 in Figure 2a). Each Raman spectrum was acquired for 120–180 s. A relatively long collection time was required because PI and PS are nonresonant at the excitation wavelength of 532 nm. The peaks were assigned by comparing their frequencies with the Raman spectra of pure PI or PS (Figure 2c).^[33,34] Characteristic bands belonging to PS at 1602 cm^{-1} (δ_{ip} (ring skeleton)) and 1002 cm^{-1} (δ_{op} (ring)) and to PI at 1664 cm^{-1} ($\nu(\text{C}=\text{C})$) were found in each spectrum. It can be observed from the variations in band intensities that the protrusions (positions 1–10) and depressions (positions 11–13) were enriched with PS and PI, respectively.

On closer scrutiny, one can see that all the spectra contain peaks from both polymers. For example, at position 12, PS signals can be detected although the illumination laser spot is entirely within a PI depression (see Figure 2a and d). Likewise, at position 8, PI signals are present although the laser spot is within a PS protrusion. This finding shows that the entire PI/PS film did not undergo full phase separation along its thickness, in contrast to a model presented in the literature.^[35]

The relative surface tensions of the polymers between themselves and with the substrate/air play a critical role for the final locations of the polymers in a spin-coated film.^[10,36] This implies that once the identities of the polymers at the interfaces are ascertained, the chemical structure of the film can be elucidated. However, confocal Raman spectroscopy, with its limited lateral (≈ 400 nm) and depth ($\approx 1 \mu\text{m}$) resolution, cannot give us more information on the chemical nature of these interfaces. This held even when the high-numerical-aperture objective was moved in the z direction to attempt “depth profiling” – no significant relative intensity variations of the PI and PS bands were observed.

2.2. TERS: Investigating the Surface and Subsurface of PI/PS Films

TERS will now be demonstrated to be a sensitive analytical technique for polymer films. The experimental conditions are similar to those of confocal Raman spectroscopy but with the addition of an Ag-coated tip contacting the sample. An SEM image of such a tip is presented in Figure 1. The lateral and depth resolutions (≈ 20 nm) afforded by the probes are known to be below the radius of curvature of the Ag nanoparticles attached to the tip apex.^[29,30,37] Sample scanning by moving the piezoelectric stage was performed so that the tip-to-laser beam alignment did not change during the experiment. Tip stability is paramount in these kinds of experiments, and tip drift was suppressed by prescanning and irradiating the tip tens of minutes before the actual measurement.^[24]

AFM topography images and TER spectra collected from PI/PS thin-film samples are presented in Figure 3. A shorter acquisition time of 60 s is sufficient, due to the TERS enhancement. The AFM image of the PI/PS film is similar to the one shown in Figure 2a. The crescents at the fringes of the protrusions are imaging artifacts that result from the slower response of the piezo sample-scanning stage. These occurred even when uncoated tips were used. Naturally, these were not present with AFM tip-scans (Figure 2a). TER spectra were acquired at many positions on this sample, but for brevity only a representative subset is shown in Figure 3b. (A large region several micrometers in length and width is presented here to show that the phenomenon is general.) The chemical fingerprints of PS and PI were reproducibly found in all the TER spectra. At first glance, the presence of a homogeneous mixture of PI and PS would be the most straightforward interpretation of the TERS data. However, the AFM image suggests otherwise, that is, the spectra have to be interpreted in the light of the known immiscibility and segregation of the polymers. Here, we postulate that the segregation is in the form of separate layers of PS and PI thin films.

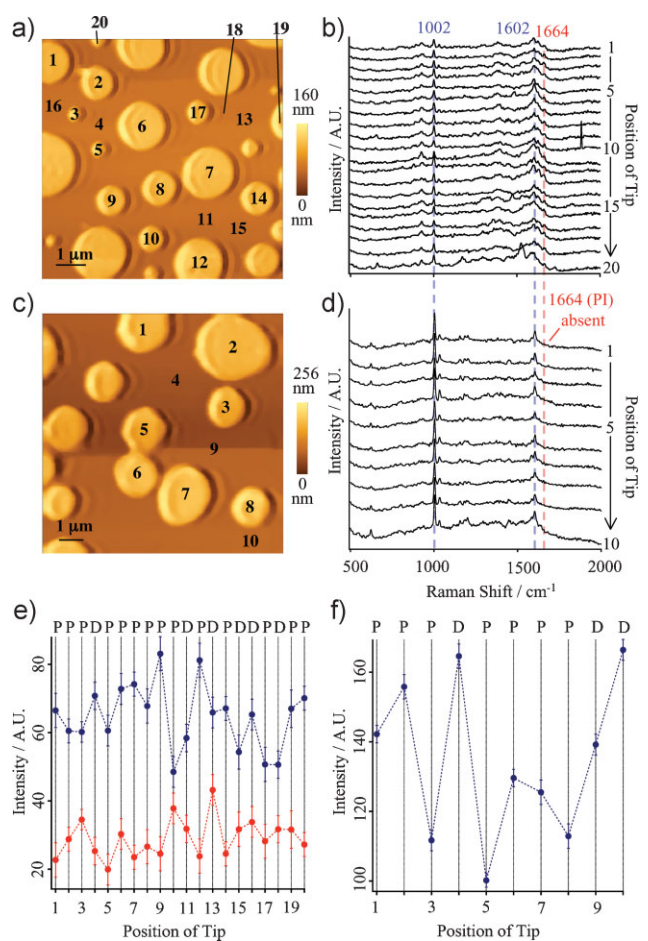


Figure 3. a) AFM topography image of a PI/PS film and b) sequence of TERS spectra collected from the positions depicted in (a). The spike in spectrum 10 was caused by cosmic rays. c) AFM topography image of a hexane-washed PI/PS film and d) sequence of TERS spectra collected from the positions depicted in (c). Each spectrum was acquired for 60 s. e, f) Intensities of the PI (1664 cm^{-1} , red trace) and PS (1002 cm^{-1} , blue trace) TER bands in (b) and (d) plotted as a function of the tip position on the sample, respectively. P and D denote protrusion and depression (on the sample), from which a TERS spectrum was measured. Signal-to-noise considerations allowed the derivation of error bars, which were added to (e) and (f). The lines that connect the data points are guides to the eye.

As a result of its lower surface tension (γ), we hypothesize that PI ($\gamma_{\text{PI}} = 32\text{ dyne cm}^{-1}$), in preference over PS ($\gamma_{\text{PS}} = 40\text{ dyne cm}^{-1}$), is enriched at the polymer/air interface of the PI/PS film. Given the depth of view (20 nm) of TERS, this also implies the presence of a continuous PS subsurface layer. To test this hypothesis, selective dissolution of the top PI layer was performed by soaking a PI/PS sample in hexane for 5 min; PS is insoluble in hexane. The sample was then dried by a N_2 gas flow. Figure 3c and d show the AFM topography and TERS spectra, respectively, collected from the washed PI/PS thin film. The overall morphology of the polymer film does not change after washing, but the acquired TERS spectra show only PS peaks. No signals from PI were found. This spectroscopic observation can only be expected if there is a continuous hexane-insoluble subsurface PS layer. To determine if this PS layer is wetting the substrate, another selective dissolution

experiment was performed. *N,N*-dimethylformamide (DMF), a solvent that dissolves only PS, was used. Upon immersion in DMF, the remaining film from a hexane-washed PI/PS sample was observed to solubilize. No topographical or Raman signals could subsequently be obtained from such a sample, which demonstrates that PS is directly in contact with the glass substrate.

2.3. TERS: Seeing More of Polymer Structures

Details of the PI/PS surface structure were also revealed by the TERS data. The intensities of the PI (1664 cm^{-1}) and PS (1002 cm^{-1}) TER bands in Figure 3b and d are plotted as a function of the tip position on the sample (Figure 3e and f, respectively). The key observation is that the intensities of the TER bands were not constant during the measurements. For example, in Figure 3e, the strength of the PS band at 1002 cm^{-1} is about 1.5 times more intense in positions 9 and 12 (both protrusions) than in positions 10 (protrusion) and 11 (depression; “observation a”). In Figure 3f, the intensity of the PS band is about 1.5 times stronger at positions 4 and 10 (both depressions) than at positions 5 or 8 (both protrusions), that is, less PS was detected in some PS-rich domains (“observation b”)! These intensity differences are significant and cannot be assigned to experimental limitations, such as laser power fluctuations.

Observation a can be partially attributed to the inhomogeneity of the polymer film on the nanometer scale, that is, the PS and PI layers are not perfectly uniform in their thicknesses. Specifically, for positions 9–12 in Figure 3e, the intensities of the PS TER signals are observed to increase when those from PI decrease (and vice versa). This happens because a thinner PI overlayer facilitates the TERS detection of more subsurface PS.

We attribute observation b to the presence of nanopores within the PS film. TERS will thus detect a lower quantity of PS in some locations. One source of these nanopores could be from encapsulated solvent or air pockets formed during the spin-coating process. Another could be from the selective dissolution in which PI trapped in the PS domain is removed. The same phenomenon was also found for an unwashed PI/PS sample, for example, a stronger PS signal at position 16 (depression) compared to 17 (protrusion) in Figure 3e. Note that the PI signal intensities actually decrease from position 16 to 17, which further confirms that this observation cannot be simply attributed to a mere difference in thickness of the PI overlayer. Porous polymer films made from selective dissolution also exhibit porous surfaces.^[32] These were not observed in our AFM topography image. We conclude from these lines of evidence that the nanopores, which are located at the subsurface, must have been formed during the spin-coating process. The purpose for presenting the intense PS signals in positions 4 and 10 (Figure 3d) is not to suggest that nanopores occur more frequently at the depressions. Rather, these data help to demonstrate the existence of the nanopores. The stronger PS intensity cannot be attributed to other causes, such as far-field contributions, since the PS layer cannot be physically thinner on a protrusion compared to a depression. This is corroborated by the confocal Raman data: stronger

far-field PS signals are obtained from protrusions than from depressions.

Using the same line of reasoning, observation b cannot be rationalized by a difference in thickness of the PS layer. The possibility of PI embedded in the PS layer (resulting in a lower PS signal) is also rejected, since there were no detectable PI TERS signals for the washed PI/PS film. In addition, the possibility of toluene being encapsulated in the polymer layer is ruled out because no toluene TERS/Raman peaks were recorded in this work. This is to be expected, as toluene has a relatively high volatility. Thus, most likely, the nanopores consist of air pockets.

2.4. TERS: Control Experiments and High Spatial Resolution Data

Care was taken throughout this work to ensure that neither tip wear nor drift occurred during spectra acquisition. These may cause artifacts in the signals, which would result in unreliable data. We present an experiment to assess these two criteria. An AFM image was taken from a PI/PS sample (Figure 4a). Five positions were selected. One spectrum was collected from each position, and this process was repeated

three more times. Hence, a total of four spectra were collected from each spot. Spectra from the first and last positions (marked as positions 1 and 2 in Figure 4a) are shown in Figure 4b. With an acquisition time of 60 s per spectrum, the fourth spectrum of each position was acquired tens of minutes after the first. Yet, the band intensities remain identical throughout for each point, which demonstrates the absence of tip wear and drift throughout the TERS measurement. It can be further observed that although the illuminated far-field region of position 1 consists of a larger PS volume (indicated by the protrusion) than that of position 2, the resultant PS intensity in the former spot is actually smaller. This finding mirrors the data shown in Figure 3f (observation b).

This control experiment was chosen, rather than SEM measurements of the tip prior to and after a TERS experiment, for two reasons. Firstly, small changes to the tip that may not be observable by SEM can have significant effects on the TERS intensities.^[23] Secondly, electron-beam-induced deposition of carbon during an SEM experiment is inevitable and would render the tip unusable for TERS.^[38] Therefore, a more reliable way of checking tip stability is by repeating TERS measurements at the same sample positions.

To demonstrate the high spatial resolutions of our measurements, AFM imaging followed by a TERS line scan of spectra with equidistant steps of 20 nm was performed on a PI/PS sample (Figure 4c and d). A large PS protrusion was sampled so that the far-field illumination would always be within it. This kept the signals of the far-field spectra at a constant level. Hence, any intensity variations found during the TERS line scan should be due to near-field effects. The red bar in the AFM image in Figure 4c indicates the positions at which the line scan was obtained. The band intensities of PI and PS are shown in Figure 4d. Intensity variations are unmistakably present, which demonstrates the capabilities of TERS for resolving nanosized compositional variations on surface of the polymer film. Moreover, a spatial resolution of ≈ 20 nm can be estimated from the intensity profile of the PS or PI signals along the line scan (Figure 4d).^[39]

The present finding (inhomogeneous polymer layer thickness and nanopores) was demonstrated by four sets of data, and the variations are clearly beyond the measurement noise. The TERS data from positions 4 and 10 in Figure 3d also demonstrate clearly that the phenomenon cannot be attributed to other causes, such as far-field contributions. The present observations are consistent with nanoscale compositional differences of spin-coated films – such inhomogeneities have been previously observed for spin-coated films of brilliant cresyl blue dyes on glass slides.^[22]

No frequency shifts of the PS or PI TER bands were found, which simplified the spectral assignment. Some spurious peaks (e.g., broad bands at $1500\text{--}1600\text{ cm}^{-1}$ in spectrum 20 of Figure 3b) were observed in the TER spectra. These were assigned to amorphous carbon, which could either be from the tip (carbon deposited during the Ag vapor coating) or from contamination on the surface of the polymer film.^[22] The possibility of PI and/or PS dissociating into amorphous carbon cannot be completely ruled out. However, this should not be a major cause of the carbon signals in our spectra, because amorphous carbon has a huge Raman scattering cross

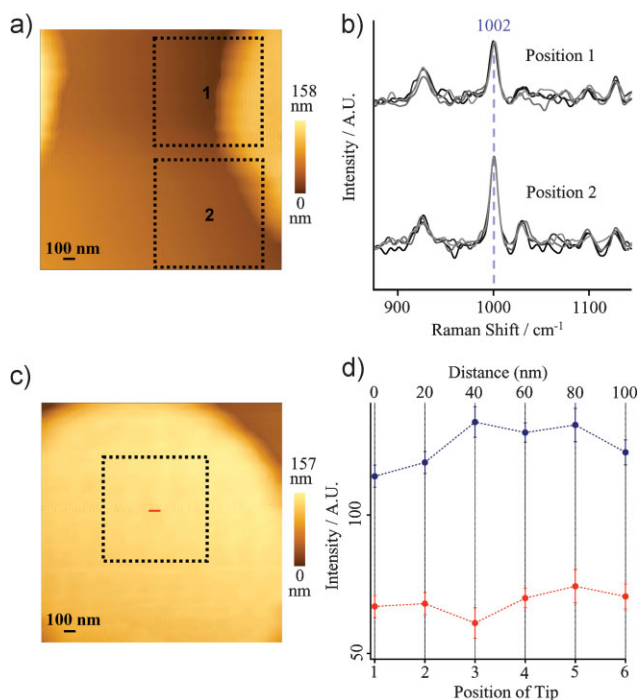


Figure 4. a) AFM topography image of a PS protrusion in a PI/PS film. b) Zoomed view of two sets of TERS spectra taken at positions 1 and 2. Each set consists of four spectra (marked by different shades of gray and black) collected at different times. c) AFM topography image of a PI/PS film. Six TERS spectra were acquired along the red bar, with an equidistant separation of 20 nm between each sample position. d) Intensities of the PI (1664 cm^{-1} , red trace) and PS (1002 cm^{-1} , blue trace) TER bands plotted as a function of the tip position on the sample. Signal-to-noise considerations allowed the derivation of error bars, which were added to (d). The dotted boxes in (a) and (c) show the maximum far-field region that weakly contributed to the overall signal during the line scan.

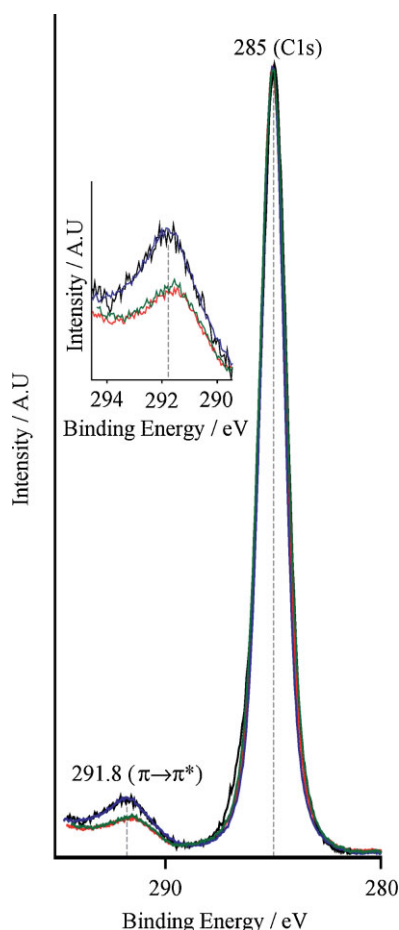


Figure 5. X-ray photoelectron spectra of polymer films. Reference PS (blue trace) and PI (red trace) films, and PI/PS film before (green) and after washing (black). Insert: zoom of the $\pi \rightarrow \pi^*$ peaks at 291.8 eV.

section.^[40] If analyte dissociation was significant, the observed carbon signals would be far more intense than the PI or PS TER signals.

The TERS tip should be free from adsorbed polymers, because this will lead to artifacts in the data. This is ensured after each experiment by collecting the tip's spectrum with an accumulation time of 120 s. No traces of PI or PS were found.

2.5. XPS Experiments of PI/PS Films

XPS was performed to corroborate the vibrational spectroscopy data. The XPS sampling depth for polymer samples is ≈ 3 nm at a takeoff angle of 0° , that is, XPS is more surface sensitive than TERS, albeit with poorer lateral spatial resolution.^[41] The XPS data are presented in Figure 5. The $\pi \rightarrow \pi^*$ shake-up peak at 291.8 eV is more intense for PS (blue trace) than PI (red trace) due to the larger number of C=C bonds in the former. As compared to the C 1s peaks, which cannot be easily resolved energetically, the $\pi \rightarrow \pi^*$ peaks can be used to identify the polymer at the film's surface.^[42] We do this by comparing the intensities of the $\pi \rightarrow \pi^*$ shake-ups of the PI/PS samples with those of pure PI and PS. The C 1s peaks are intensity-normalized and, to correct for charging effects,

were normalized to 285 eV. For an unwashed PI/PS sample, its $\pi \rightarrow \pi^*$ shake-up (green trace) has an intensity which matches that of PI, thus indicating that PI is at its surface. Moreover, the thickness of the top PI layer has to be >3 nm. After selective dissolution of PI with hexane, the $\pi \rightarrow \pi^*$ shake-up (black trace) of the washed PI/PS matches that of PS, thus showing that PS is at the subsurface. If this continuous subsurface phase described above did not exist or was mixed with PI, the $\pi \rightarrow \pi^*$ peak would most likely have an intensity in between that of pure PS and PI.

3. Discussion

3.1. Surface Structure of the PI/PS Film

The structure of the PI/PS film that can be constructed from the data is illustrated in Figure 6. It consists of a PI and PS film at the surface and subsurface, respectively. The continuous PS subsurface has never been identified in previous studies of PI/PS films. The film formation mechanism is postulated as follows. At the beginning of the spin-coating process, most of the toluene evaporates leaving a thin layer on the substrate. As the polymer solution thins due to fluid flow, its viscosity increases, which reduces shear thinning of the film. Phase separation of the PI and PS occurs at these later stages of the spin-coating process. As the solvent evaporates further,

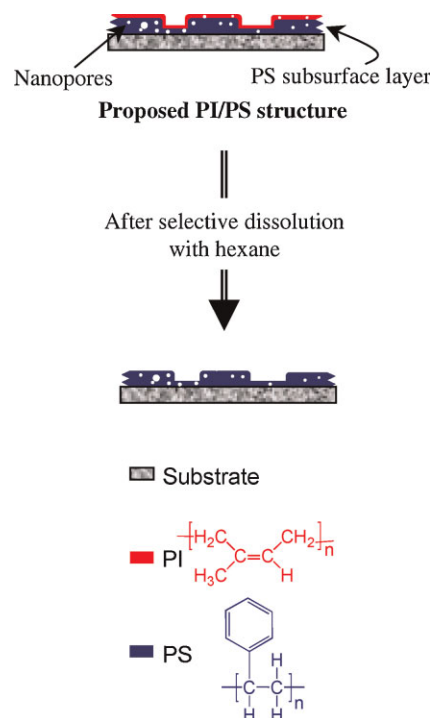


Figure 6. Schematic diagram of the proposed structure of the PI/PS film. The PS domains are linked by a continuous PS subsurface layer. The surface of the film is completely covered with a layer of PI. After selective dissolution of the PI overlayer, the subsurface PS is exposed. The nanopores are also depicted. The thicknesses of the PI and PS layers are not to scale and the edges of the polymer films are left uncompleted, as these were not experimentally measured in this work. The chemical structures of PI and PS are shown.

the development of distinct PS domains of different sizes occurs. This is followed by the collapse of the PS domains on the substrate. PS wets the substrate, as demonstrated by TERS (only PS signals seen from a hexane-washed PI/PS sample), selective dissolution (no film remaining on the substrate after consecutive hexane/DMF washing), and XPS (only PS seen from a hexane-washed PI/PS sample). This is also consistent with the presence of PI at the polymer film surface, which is in agreement with its lower surface tension as compared to PS. The propensity for nanopore formation is ascribed to the poor miscibility of the PI and PS, as well as the high volatility of the toluene solvent.^[5] Porous polymer films are usually fabricated by selectively dissolving a component of a phase-separated polymer-blend film. Our TERS results indicate that such films can be alternatively and easily formed by spin-coating of an incompatible polymer mixture, such as PI/PS.

The PI layer on top of the PS is expected to have a thickness t of $3 < t_{PI} < 20$ nm. This is because a thicker layer would prevent the TERS detection of subsurface PS, whereas a thinner one would be inconsistent with the XPS data. Considering the heights of the PS domains of 150–300 nm and to satisfy the 1:1 weight stoichiometry of the samples, the question about the whereabouts of the extra PI arises. One possible location of the PI is at the fringes of the film. Since PS domains were formed in a PI matrix during the spin-coating process, it would not be unusual to find a higher concentration of PI at the edges of the film where shear-force effects are the largest.

3.2. TERS of Polymer Films: Experimental Insights

The TERS data are the key to the model: PI and PS films were not only identified at the surface and subsurface, respectively, but also inhomogeneities in their thickness and the presence of subsurface nanopores were elucidated. All these data were obtained with high spatial resolutions, without using fluorescent labels or special operating conditions, such as high vacuum (necessary for XPS). It is also highlighted here that PI and PS are weak scatterers and are nonresonant with 532 nm excitation. Such important samples that are, however, poor Raman scatterers have hardly been studied by TERS.^[13]

Although AFM, confocal Raman spectroscopy, selective dissolution, and XPS were employed to give corroborating evidence in this work, their data cannot fully substitute those of TERS. Assuming that only these methods (except TERS) are available, the best model that could be derived is the vertical and lateral phase separation of the polymers. PI and PS will be identifiable at the surface and subsurface. However, spatially resolved information on local film thicknesses cannot be obtained. Similarly, the detection of the presence of nanopores is a unique capability of TERS. In short, the clear-cut chemical identification of local structural differences cannot be easily made by any other methods. This has also been previously demonstrated by findings obtained from TERS studies of carbon nanotubes.^[21,23]

Consecutive TER and far-field Raman spectra could not be acquired from the same spot during a mapping experiment (see the Experimental Section). However, the general enhancement afforded by the TERS tips was estimated by

performing “tip engaged–tip retracted” measurements on the samples. A signal contrast of at least $>2\times$ is observed. Taking into account the difference in area of the far-field and near-field regions, the net enhancement is estimated to be 10^3 – 10^4 .

The fact that PI has peaks that are weak even on the unwashed PI/PS sample suggests that a reduction by a factor of 10 after washing may render it undetectable in Figure 3d. However, in these cases of incomplete dissolution, we have observed patches of PI in the AFM images (data not shown). These were not found in Figure 3c. Our interpretation of the absence of PI would also be subsequently confirmed by XPS (Section 2.5).

The TER intensity variations exhibited in this work cannot be ascribed to a) tip drift and/or b) physical and chemical changes to the enhancing nanoparticles. The former was ruled out experimentally in Section 2.4. Moreover, tip drift usually causes a steady decrease in signal intensity, that is, with time the tip usually drifts further away from its optimum position with respect to the laser focus. Drift induced by laser-induced heating is unlikely because a modest laser power was used for illumination. Furthermore, (b) usually leads to either a very dramatic fluctuation or a steady decrease of the TERS intensities (from alteration of the enhancing properties of the tip).^[24,43] Neither of these phenomena was observed in the present work.

The ability to acquire high-quality TER spectra from a nonresonant Raman-active PI/PS sample occurs through a combination of efforts, from judicious tip preparation to proper control of the laser power and spectra collection time. The TERS data were reproduced several times. This demonstrates that although the precise shape of the Ag nanoparticles formed at the AFM tip apex is difficult to control, the spatial resolution afforded by TERS is constant and is thus reliable.^[25] If this was not the case, the occasional absence of PS peaks would be expected in the TERS of PI/PS samples (due to smaller depth resolution).

3.3. The TERS Approach in the Analysis of Polymer Surfaces

We have demonstrated that TERS is a suitable nanoanalytical technique for investigating the surfaces of polymer films. In the future, the investigation of organic LED samples will be of special interest. TERS of these polymer-based devices is expected to be easier than the present study on PI/PS. This is because many of them will exhibit resonance Raman enhancement with visible-light excitation. The time required to acquire a TER spectrum will therefore be significantly shortened, which facilitates rapid TER microscopy. Knowledge of polymer morphology is essential in custom-designing the electronic and light-emitting properties of LEDs.^[3,44] Since these films are usually tens of nanometers in thickness, confocal Raman spectroscopy will not be as useful for surface chemical analysis as compared to TERS.^[19]

The ability of TERS to detect subsurface nanopores in a sample with high spatial resolution has obvious applications in nanotechnology.^[5] Nanopores, if they are extended to the surface, are usually imaged by AFM topographical scans. In the present work, the presence of subsurface nanopores in the

PI/PS films could be further verified by performing SEM on cross sections (microtomes) of the cryo-frozen samples. However, the ability of SEM to discern nanopores in a heterogeneous (two or more components) polymer blend is more difficult, because SEM contrast does not allow the chemical identity of the analyte to be elucidated.

Finally, we highlight the multimethod approach used in this work. Presently, only a handful of research groups have performed chemical analysis with TERS.^[13] It is usually used alone without corroborative evidence from other methods. To the best of our knowledge, the only company that has employed TERS for its purposes is the microchip producer AMD, albeit for research and not for diagnosis of commercial products.^[45] In this work, the TERS results were compared with data collected independently through several established analytical methods: AFM, confocal Raman spectroscopy, selective dissolution, and XPS. The consistency of all the data demonstrates that TERS is on the way to achieving maturity as a nanoanalytical technique. We envisage TERS to be a superior analytical method over the commonly used AFM because it gives chemical and morphological information simultaneously.

4. Conclusions

Significant steps have been taken for the first time to establish TERS as a unique analytical technique for polymer thin films. High-quality TER spectra were obtained from a nonresonant Raman-active PI/PS polymer-blend thin film. PI and PS were identified at the surface and subsurface, respectively. Differences in local thickness of the PI and PS layers, as well as nanopores at the subsurface of the polymer film, have also been found. The surface sensitivity of TERS facilitated the facile and unambiguous structure elucidation of the polymer film. This could not be otherwise performed by conventional analytical methods, such as AFM, confocal Raman spectroscopy, or XPS. The ability of TERS to accomplish label-free, chemically specific subsurface detection will also contribute greatly towards the understanding of biological processes and characterization of microelectronic devices.

5. Experimental Section

Sample preparation: PI (molecular weight M_w 200 000, 1,4-polyisoprene GPC standard, Fluka) and PS (M_w 43 009, GPC standard, Aldrich) were used as samples. Each polymer (20 mg) was dissolved in toluene (1 mL). Thin PI/PS films were prepared by spin-coating of a 1:1 polymer solution mixture (2 μ L) onto either clean glass slides or Si wafers. The surface chemistry of the substrate does not affect the overall phase morphology.^[35] Measurements were taken only near the center of the spin-coated films so that the effect of shear forces on phase separation was not an important factor.

TERS and confocal Raman spectroscopy: The home-built setup consisted of an LSCM (IX 70, Olympus, Japan), an AFM instrument

(Explorer, Veeco, USA), and a Raman spectrograph/CCD detector (Holospec, Kaiser, USA).^[20] The sample was fixed onto an XYZ piezoelectric stage (P-500, Physik Instrumente, Germany) mounted above the microscope. A 1.4 NA oil-immersion objective was used to focus light from a 532 nm continuous-wave laser (Ventus, Laser Quantum, UK) onto the samples. Backscattered light was collected through the same objective and channeled either to the photomultiplier tube for confocal imaging or to the Raman spectrograph. All the experiments were performed under ambient conditions.

The TERS tips were fabricated by vapor-coating SiN AFM contact tips (RC800PSA, Olympus, Japan) with AlF₃ (20 nm), followed by Ag (30 nm).^[22] To reduce carbon contamination signals from prolonged laser irradiation, the galvanic mirrors of the LSCM scanned the laser beam rapidly around the tip over an area of 900 × 900 nm². Nonetheless, it was not possible to prevent the appearance of carbon signals in some of the TER spectra. The spectra with huge carbon bands were not included in the data analysis.

A characteristic of *continuous* TERS measurements (using trigger pulses) is that a far-field Raman spectrum cannot be collected after each TER spectrum. This is because the tip would have to be retracted.^[22,46] The implication is that the degree of near-field enhancement cannot be easily determined as done in “tip-engaged followed by tip-retracted” experiments. To ensure that the signals were largely caused by tip enhancement, we checked their intensities when the tip was on a protrusion or depression. If the signals had originated from the far field, a stronger PS (or PI) signal when the tip was on the protrusion (or depression) would always be expected. These correlations were not observed in the TERS measurements. This demonstrates that the signals were a consequence of tip enhancement.

No background subtraction or smoothing of the spectra was made. The data points were processed using Igor Pro Version 4.09A.

XPS: The surface chemical composition of the polymer films was measured at room temperature using a Sigma Probe (Thermo, Scientific) equipped with a hemispherical analyzer. The instrument was operated in the large-area mode by using the MgK α source at 100 W. The spectra were recorded at a takeoff angle of 90°. The pressure of the chamber was maintained below 10⁻⁸ mbar during the measurements. Detail spectra were acquired with a pass energy of 25 eV, a dwell time of 50 ms, and at an energy step of 0.05 eV.

Acknowledgements

We thank the Electron Microscopy Center at ETH Zurich (EMEZ), and Frank Krumeich for performing the SEM analyses.

[1] R. A. Segalman, *Mater. Sci. Eng. R* **2005**, *48*, 191–226.

[2] R. Jones, *Phys. World* **1995**, *8*, 47–51.

[3] J. J. M. Halls, C. A. Walsh, N. C. Greenham, E. A. Marseglia, R. H. Friend, S. C. Moratti, A. B. Holmes, *Nature* **1995**, *376*, 498–500.

- [4] C. Ton-That, A. G. Shard, D. O. H. Teare, R. H. Bradley, *Polymer* **2001**, *42*, 1121–1129.
- [5] K. Norrman, A. Ghanbari-Siahkali, N. B. Larsen, *Annu. Rep. Prog. Chem. Sect. C: Phys. Chem.* **2005**, *101*, 174–201.
- [6] S. Walheim, E. Schaffer, J. Mlynek, U. Steiner, *Science* **1999**, *283*, 520–522.
- [7] E. Moons, *J. Phys. Condens. Matter* **2002**, *14*, 12235–12260.
- [8] O. P. Behrend, L. Odoni, J. L. Loubet, N. A. Burnham, *Appl. Phys. Lett.* **1999**, *75*, 2551–2553.
- [9] M. F. Paige, *Polymer* **2003**, *44*, 6345–6352.
- [10] P. Wang, J. T. Koberstein, *Macromolecules* **2004**, *37*, 5671–5681.
- [11] C. A. Michaels, X. H. Gu, D. B. Chase, S. J. Stranick, *Appl. Spectrosc.* **2004**, *58*, 257–263.
- [12] M. B. Raschke, L. Molina, T. Elsaesser, D. H. Kim, W. Knoll, K. Hinrichs, *ChemPhysChem* **2005**, *6*, 2197–2203.
- [13] T. Schmid, B. S. Yeo, W. Zhang, R. Zenobi, in *Tip Enhancement: Advances in Nano-Optics and Nano-Photonics*, (Eds.: S. Kawata, V. M. Shalaev), Elsevier, Amsterdam **2007**, pp. 115–155.
- [14] T. Taubner, R. Hillenbrand, F. Keilmann, *Appl. Phys. Lett.* **2004**, *85*, 5064–5066.
- [15] C. A. Michaels, D. B. Chase, S. J. Stranick, in *Applications of Scanned Probe Microscopy to Polymers*, Vol. 897 (Eds.: J. D. Batteas, C. A. Michaels, G. C. Walker), American Chemical Society, Washington **2005**, pp. 38–50.
- [16] U. Schmidt, S. Hild, W. Ibach, O. Hollricher, *Macromol. Symp.* **2005**, *230*, 133–143.
- [17] C. Sammon, C. Mura, P. Eaton, J. Yarwood, *Analisis* **2000**, *28*, 30–34.
- [18] H. Reinecke, S. J. Spells, J. Sacristan, J. Yarwood, C. Mijangos, *Appl. Spectrosc.* **2001**, *55*, 1660–1664.
- [19] P. K. H. Ho, J. S. Kim, J. H. Burroughes, H. Becker, S. F. Y. Li, T. M. Brown, F. Cacialli, R. H. Friend, *Nature* **2000**, *404*, 481–484.
- [20] C. Vannier, B. S. Yeo, J. E. Melanson, R. Zenobi, *Rev. Sci. Instrum.* **2006**, *77*, 023104.
- [21] N. Anderson, P. Anger, A. Hartschuh, L. Novotny, *Nano Lett.* **2006**, *6*, 744–749.
- [22] B. S. Yeo, T. Schmid, W. Zhang, R. Zenobi, *Anal. Bioanal. Chem.* **2007**, *387*, 2655–2662.
- [23] A. Hartschuh, E. J. Sanchez, X. S. Xie, L. Novotny, *Phys. Rev. Lett.* **2003**, *90*, 095503.
- [24] W. H. Zhang, T. Schmid, B. S. Yeo, R. Zenobi, *J. Phys. Chem. C* **2008**, *112*, 2104–2108.
- [25] B. S. Yeo, W. Zhang, C. Vannier, R. Zenobi, *Appl. Spectrosc.* **2006**, *60*, 1142–1147.
- [26] P. L. Stiles, J. A. Dieringer, N. C. Shah, R. P. Van Duyne, *Annu. Rev. Anal. Chem.* **2008**, *1*, 601–626.
- [27] K. F. Domke, D. Zhang, B. Pettinger, *J. Am. Chem. Soc.* **2006**, *128*, 14721–14727.
- [28] N. Hayazawa, Y. Inouye, Z. Sekkat, S. Kawata, *Chem. Phys. Lett.* **2001**, *335*, 369–374.
- [29] M. Micic, N. Klymyshyn, Y. D. Suh, H. P. Lu, *J. Phys. Chem. B* **2003**, *107*, 1574–1584.
- [30] N. L. D. Mehtani, R. D. Hartschuh, A. Kisliuk, M. D. Foster, A. P. Sokolov, J. F. Maguire, *J. Raman Spectrosc.* **2005**, *36*, 1068–1075.
- [31] L. A. Utracki, in *Polymer Blends Handbook*, (Ed.: L. A. Utracki), Kluwer Academic, Dordrecht **2003**, pp. 1–122.
- [32] R. H. Schmidt, K. Mosbach, K. Haupt, *Adv. Mater.* **2004**, *16*, 719–722.
- [33] S. W. Cornell, J. L. Koenig, *Macromolecules* **1969**, *2*, 546–549.
- [34] R. A. Nyquist, C. L. Putzig, M. A. Leugers, R. D. McLachlan, B. Thill, *Appl. Spectrosc.* **1992**, *46*, 981–987.
- [35] A. Budkowski, A. Bernasik, P. Cyganik, J. Raczowska, B. Penc, B. Bergues, K. Kowalski, J. Rysz, J. Janik, *Macromolecules* **2003**, *36*, 4060–4067.
- [36] K. Dalnoki-Veress, J. A. Forrest, J. R. Stevens, J. R. Dutcher, *Physica A* **1997**, *239*, 87–94.
- [37] J. J. Wang, Y. Saito, D. N. Batchelder, J. Kirkham, C. Robinson, D. A. Smith, *Appl. Phys. Lett.* **2005**, *86*, 263111.
- [38] A. E. Vladar, M. T. Postek, R. Vane, *Proc. SPIE* **2001**, *4344*, 835–843.
- [39] W. H. Zhang, T. Schmid, B. S. Yeo, R. Zenobi, *Israel J. Chem.* **2007**, *47*, 177–184.
- [40] J. C. Tsang, J. E. Demuth, P. N. Sanda, J. R. Kirtley, *Chem. Phys. Lett.* **1980**, *76*, 54–57.
- [41] P. J. Cumpson, *Surf. Interface Anal.* **2001**, *31*, 23–34.
- [42] J. A. Gardella, S. A. Ferguson, R. L. Chin, *Appl. Spectrosc.* **1986**, *40*, 224–232.
- [43] A. Kudelski, B. Pettinger, *Chem. Phys. Lett.* **2000**, *321*, 356–362.
- [44] M. Berggren, O. Inganas, G. Gustafsson, J. Rasmussen, M. R. Andersson, T. Hjertberg, O. Wennerstrom, *Nature* **1994**, *372*, 444–446.
- [45] L. Zhu, C. Georgi, M. Hecker, J. Rinderknecht, A. Mai, Y. Ritz, E. Zschech, *J. Appl. Phys.* **2007**, *101*, 104305.
- [46] E. Bailo, V. Deckert, *Angew. Chem.* **2008**, *120*, 1682–1685; *Angew. Chem. Int. Ed.* **2008**, *47*, 1658–1661.

Received: July 29, 2008
Revised: December 1, 2008
Published online: March 4, 2009